



ELSEVIER

Physica A 281 (2000) 337–347

PHYSICA A

www.elsevier.com/locate/physa

The surface properties of a van der Waals fluid

Nicolas G. Hadjiconstantinou^{a,*}, Alejandro L. Garcia^{b,1},
Berni J. Alder^a

^a*Lawrence Livermore National Laboratory, Livermore, CA 94551, USA*

^b*Center for Computational Sciences and Engineering, Lawrence Berkeley National Laboratory,
Berkeley, CA 94720, USA*

Abstract

Surface properties are obtained from an extension of the direct simulation Monte Carlo algorithm to a hard sphere system with an infinite range, weak attractive potential that obeys the van der Waals equation of state. Liquid–vapor surface tension measurements both with and without a gravitational field are in agreement with models summarizing experimental values for simple substances. These measurements are also in agreement with the van der Waals predictions using the measured interface density profile provided the square gradient term identification with a divergent free energy expansion is ignored. The divergent term should be replaced by one that takes into account the work required to form the density gradient in the reference hard sphere system. © 2000 Elsevier Science B.V. All rights reserved.

1. Introduction

The mean field van der Waals (vdW) model has been popular because it is simple enough to be rigorously derivable from statistical mechanics, yet realistic enough to capture both the liquid and vapor states of matter, as well as predict the coexistence region by the use of the Maxwell construction. However, theoretical studies have so far been unable to predict rigorously the surface properties of the vdW model without resorting to approximations. Surface tension theories [1] require either information about the density gradient through the liquid–vapor interface or knowledge of the radial distribution function in that region. For the vdW model this information cannot

* Corresponding author. Permanent address: Mechanical Engineering Department, Massachusetts Institute of Technology, Cambridge, MA 02139, USA.

¹ Permanent address: Physics Department, San Jose State University, San Jose, CA 95192, USA.

E-mail address: algarcia@wenet.net (A.L. Garcia)

be obtained experimentally since real fluids only approximately correspond to this model.

Numerically, a vdW fluid is difficult to simulate rigorously by molecular dynamics because the particle interaction consists of a hard sphere repulsion with a weak, long-ranged attraction [2]. Recently, it was shown that the direct simulation Monte Carlo (DSMC) procedure can be generalized to the simulation of dense hard sphere systems [3], which in turn can further be extended to the simulation of the van der Waals equation of state [4]. It has thus become possible for the first time to obtain the density profile through the interface and the surface tension of a true vdW fluid and to compare these measurements with theoretical predictions.

2. DSMC extension to the vdW Fluid

For completeness, the simulation algorithm is outlined briefly. For details on DSMC, see Refs. [5,6]; extensions to higher densities are described in Refs. [3,4,7]. The fluid is represented as a collection of particles, specified by their positions, $\{\mathbf{r}_i\}$, and velocities, $\{\mathbf{v}_i\}$. At each time step, these particles are sorted into spatial cells; the dimensions of a cell are a fraction of a mean free path [8]. The number of collisions that occur within a cell during a time step τ is computed from the hard sphere collision rate, $\Gamma = \Gamma_B(n, T)Y(n)$, where n is the number density, T is the temperature, Γ_B is the Boltzmann (i.e., dilute gas) collision rate and Y is the Enskog factor that rigorously gives the collision rate in a dense gas [9]. For the simulations presented here τ is one-tenth of the mean free time. Random collision partners are selected within a cell given the hard sphere collision probability $\mathcal{P}(\mathbf{v}_i, \mathbf{v}_j) = |\mathbf{v}_r| / \sum_{i,j} |\mathbf{v}_r|$, where $\mathbf{v}_r = \mathbf{v}_i - \mathbf{v}_j$ and the sum is over eligible partners. The post-collision velocities, \mathbf{v}'_i and \mathbf{v}'_j , conserve momentum and energy. The post-collision relative velocity is chosen statistically as $\mathbf{v}'_r = |\mathbf{v}_r| \hat{R}$ where \hat{R} is a unit vector with random direction, uniformly distributed on the unit sphere.

To obtain the vdW equation of state, each pair of colliding particles is assigned a displacement \mathbf{d} . Specifically,

$$\mathbf{d}_i = \frac{\mathbf{v}'_r - \mathbf{v}_r}{|\mathbf{v}'_r - \mathbf{v}_r|} \left(\sigma - \frac{a\sigma}{b_2 Y k T} \right), \quad \mathbf{d}_j = -\mathbf{d}_i, \quad (1)$$

where k is Boltzmann's constant, a is the van der Waals attraction coefficient, $b_2 = \frac{2}{3} \pi \sigma^3$, and σ is the hard sphere diameter. For the results presented here $m = k = \sigma = a = 1$. After all collisions have been processed, each particle is moved ballistically so $\mathbf{r}_i(t + \tau) = \mathbf{r}_i(t) + \mathbf{v}_i(t)\tau + \frac{1}{2} \mathbf{a}\tau^2 + \mathbf{d}_i$ and $\mathbf{v}_i(t + \tau) = \mathbf{v}_i(t) + \mathbf{a}\tau$ where \mathbf{a} is the acceleration of an applied, external field.

The collision process outlined above results in a virial that leads to the van der Waals equation of state [9]

$$P(n, T) = nkT \left(1 + b_2 n Y(n) - \frac{an}{kT} \right). \quad (2)$$

If in the calculation of Y and d the mean density is used in each cell then (2) is exactly reproduced [4], however, at densities in the vdW loop region only the homogeneous state is found since the displacement is independent of location in the fluid. Thus, strictly speaking, in the mean field approximation no surface is obtained.

To generate coexisting phases at different densities requires having Γ and d evaluated using the local density, that is, density fluctuations must be allowed. In this model, these density fluctuations are entirely due to the repulsive hard sphere density fluctuations. Allowing density fluctuations, however, for reasons that are not entirely understood, leads to a nonlinear coupling between the displacement and the collision rate, resulting in an unphysical correlation that manifests itself as a stratification of the density aligned with the collision cells. This correlation results in a discrepancy between the correct equation of state, Eq. (2), and the measured equation of state. Unfortunately, although this discrepancy is small in absolute terms, it is of the same order as the capillarity generated pressure differences at liquid–vapor coexistence. To break up this artificial correlation an additional displacement of σ in a random direction is given to each colliding particle. This modifies the transport properties but has no effect on the equation of state [4]. The introduction of this random displacement, however, has the effect of smearing the fluid vapor–liquid interface, and leads to the largest source of uncertainty in the results. This uncertainty has been accounted for in the error bars of the quantitative results presented and in no way can change the qualitative conclusions.

Simulations initially at a density in the two phase region evolve to form drops at the correct tie-line liquid density, n_ℓ , with the remainder of the material at the saturated vapor density, n_v . However, an initially uniform density distribution does not phase separate into drops and vapor during reasonable running times unless an initial high-density region is present to nucleate the phase separation. Dense regions, initially at half the liquid density, have been observed to successfully evolve to drops; the exact size of the initial state required for nucleation is still under investigation. Fig. 1 shows the coagulation and relaxation of two proto-droplets into the equilibrium circular configuration. In this constant temperature simulation ($T/T_c = 0.756$, where T_c is the critical temperature) the initial density is 0.48 within the droplets, and 0.10 elsewhere. The final densities inside and outside the drop are very nearly the equilibrium coexistence liquid and vapor densities of $n_\ell = 0.63$ and $n_v = 0.03$.

3. Measurement of surface tension

3.1. Laplace approach

A series of simulations at varying temperatures close to the critical point is performed. A single droplet of initial density $n = 0.48$ is placed in a vapor bath of density $n = 0.1$. The temperature is held fixed by use of a thermostat in which particle velocities are adjusted locally. The system is equilibrated for at least 5000 collision times (usually

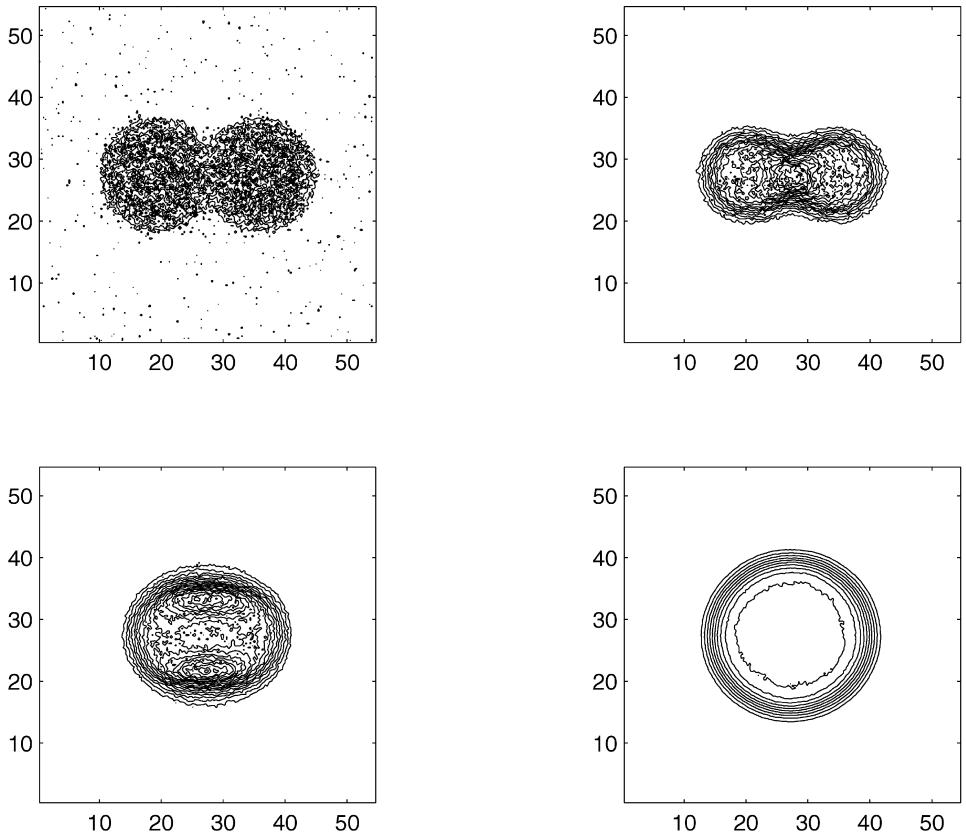


Fig. 1. Snapshots of the time evolution of two proto-droplets in a vapor bath to a circular drop. The simulation box is rectangular ($54.6\sigma \times 54.6\sigma \times 2.7\sigma$) with 4×10^5 particles. Density contours are shown starting at $n = 0.05$ in increments of 0.1; snapshots are at 2, 100, 300, and 5000 collision times.

9000) before statistical samples are gathered. The size of the simulation domain in the x and y directions is 54.6σ and contains 4×10^5 particles. The drops are between 20σ and 30σ in diameter.

The surface tension of the circular drops is calculated using the Laplace equation (in two dimensions)

$$P_d = P_\infty + \frac{\gamma}{R}, \quad (3)$$

where P_d is the pressure in the interior of the drop and P_∞ is the pressure in the ambient vapor far away from the drop. The radially symmetric pressure is calculated as the flux of normal momentum through small test areas. Typical pressure and density profiles are shown in Fig. 2. In this figure the vdW loop is evident from the variation in pressure through the interface. The definition of an equimolar radius [1] (modified

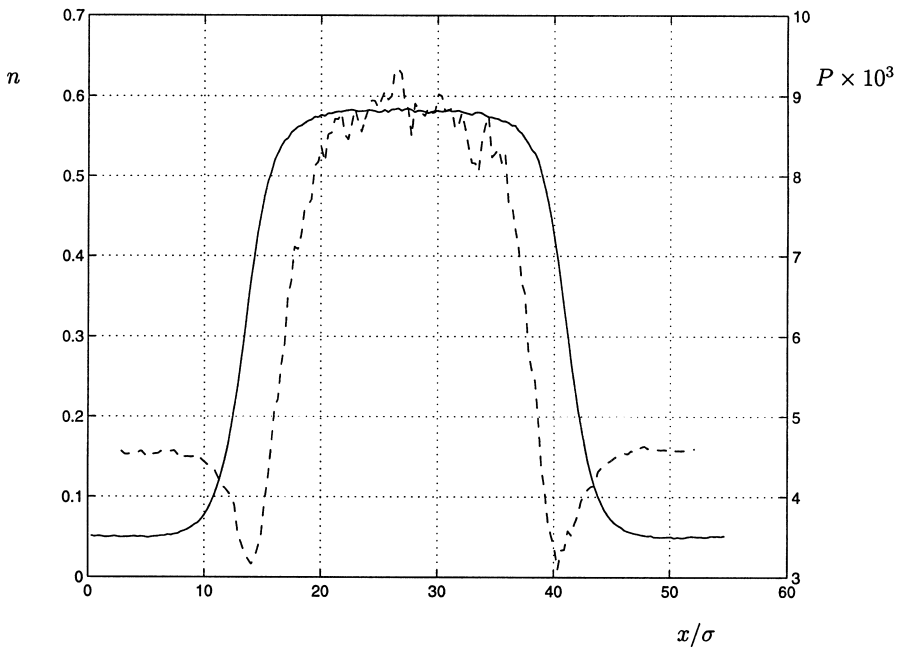


Fig. 2. Density (solid line) and pressure (dashed line), in reduced units, across a system of total width 54.6σ held at $T/T_c = 0.8$.

for two dimensions)

$$r_e^2 = \frac{1}{n_\ell - n_v} \int_0^\infty r^2 \frac{dn}{dr} dr \tag{4}$$

can be shown to be approximately equivalent to the radius at which the density reaches the value $n(R) = n_v + 0.4(n_\ell - n_v)$; this definition of the drop radius R has been subsequently used. The surface thickness, δ , has been defined as

$$\delta = -(n_\ell - n_v) \left[\frac{dr}{dn} \right]_{r=R} \tag{5}$$

The values of δ , R , and γ are given in Table 1. The drops are large enough that Tolman size corrections due to surface curvature are smaller than the simulation error bars [10]. The curvature also leads to an increase in the vapor pressure by a factor of $e^{\gamma/nmRkT}$, as predicted by the Kelvin equation [1]. This effect is always less than 15% and hence it was not explicitly accounted for, but rather included in the error estimates. An other source of error is the fairly sluggish equilibration dynamics close to the equilibrium coexistence densities.

The interface thickness is observed to be a monotonically increasing function of temperature and independent of the computational domain size, within statistical error bars, when the domain size is doubled. The long-range potential of the vdW model has

Table 1

Surface tension as a function of temperature computed from the Laplace equation (γ_L), from Elsner's method (γ_e), and the vdW theory (γ_{vdW}). The interface thickness (δ), and drop radius (R) are also shown

T/T_c	R	δ	$\gamma_L \times 10^2$	$\gamma_e \times 10^2$	$\gamma_{vdW} \times 10^2$
0.889	12 ± 1	7.5 ± 0.6	1.1 ± 0.5	2.4	2 ± 0.5
0.844	13.5 ± 1	6 ± 0.6	3.1 ± 0.4	3.9	3.1 ± 0.8
0.800	14 ± 1	5 ± 0.6	5.6 ± 1	5.6	4.4 ± 1
0.756	11.5 ± 1	5 ± 0.6	8.9 ± 1.5	7.5	6.6 ± 1
0.756	14.5 ± 1	4.5 ± 0.6	9.4 ± 1.5	7.5	5.9 ± 1
0.711	11.5 ± 1	4.5 ± 0.6	12.5 ± 3	9.4	8.7 ± 1
0.711	15 ± 1	4 ± 0.6	12.5 ± 3	9.4	7.8 ± 1

the effect of damping out capillary waves and possibly any associated divergence in the thickness [14]. If any divergences in the thickness due to the long-range potential itself are present they were not observed in the numerical experiments [13].

3.2. Mechanical approach

An independent estimate of the surface tension was obtained from its mechanical definition. Previous studies have shown that a constant external body force, such as gravity, facilitates the phase separation into liquid and vapor for a fluid in the two-phase region [4]. When a spatially varying gravitational field is introduced the liquid–vapor interface becomes curved and from this curvature the surface tension can be measured. One of the simplest ways to achieve this is spinning the fluid in a gravitational field. A variant that makes the computations significantly more tractable is to introduce a lateral “centrifugal” acceleration that is a linear function of the distance from the center of the simulation box (at $x = 0$), that is, $a_x = \omega^2 x$. This external field, in conjunction with a constant gravitational field ($a_y = -g$) in the vertical (y -direction), reproduces solid body rotation in a two-dimensional configuration. The simulations presented here are three-dimensional but shallow in the z -direction, which results in significant computational savings. The fluid reaches hydrostatic equilibrium in this field while the temperature is held fixed by use of a thermostat.

Fig. 3 shows a typical density profile from the simulations. The surface tension is calculated by applying momentum conservation in the y -direction on the control volume shown in the same figure. By momentum balance,

$$2\gamma \cos \theta = \int_1 P dA + \int \rho g dV - \int_2 P dA. \quad (6)$$

Each term on the r.h.s., as well as the interface angle θ , can be evaluated from the simulation data. Note that to avoid edge effects, the control volume is constructed such that its sides are sufficiently far away from the specular walls bounding the fluid. Faces 1 and 2 are placed optimally such that the area integrals in (6) are as accurate as possible. The interface angle θ tends toward a preferred “contact” angle between wall,

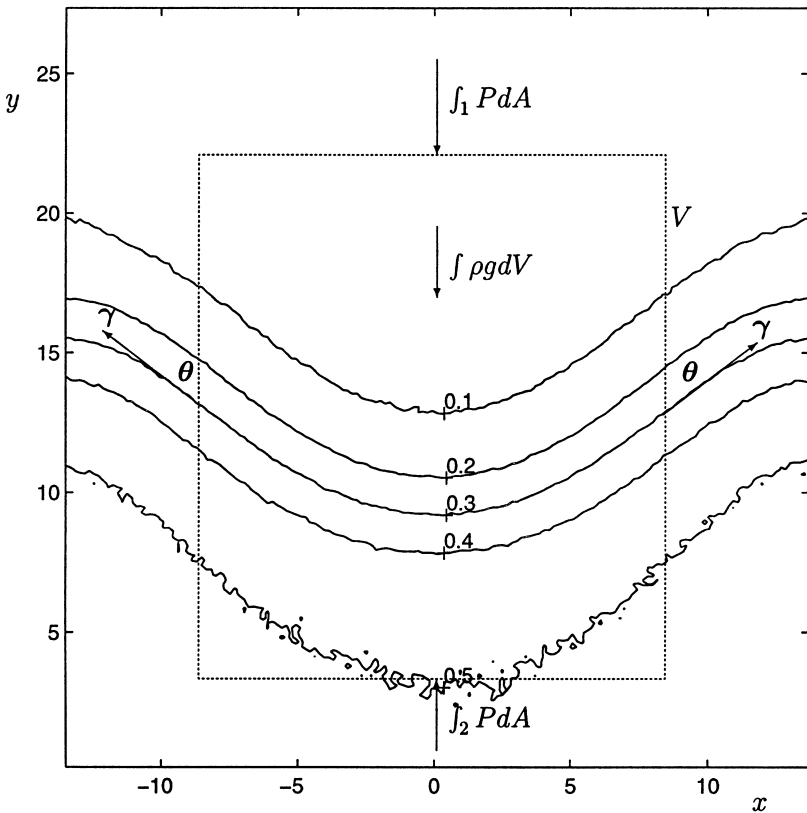


Fig. 3. Number density versus position at $T/T_c = 0.89$ for $g = 2.82 \times 10^{-4}$ and $\omega = \sqrt{4g}$. Surface tension angle, θ , is obtained from the $n = 0.3$ contour; the control volume is outlined by the dashed rectangle. The simulation box measures 27.3σ in both the x - and y -direction and contains 4×10^5 particles.

liquid and vapor and since this contact angle is not known a priori for this system, the sides of the control volume are placed away from the sides of the simulation box while maintaining a control volume sufficiently large. The pressure integrals are evaluated by measuring the net momentum transfer through faces 1 and 2.

The surface tension obtained through this method depends on the magnitude of the applied gravity as given by the Bond number, $Bo = m\bar{n}g\delta^2/\gamma$, where \bar{n} is the mean simulation density. For $Bo \geq 1$, it appears that gravity has an effect on the surface tension of the interface and the interface thickness. Unfortunately, the accuracy of the results for $Bo \geq 1$ is insufficient to allow any firm conclusions to be drawn: compressibility effects become important, and the relative importance of the left-hand side of Eq. (6) with respect to the right-hand side decreases proportionally to Bo making the results susceptible to significant error. Table 2 shows that interface thickness and surface tension are consistent with the droplet simulation results when $Bo < 1$.

Table 2

Surface tension and surface thickness computed from surface curvature for $T/T_c=0.89$. The effective rotation rate is $\omega = \sqrt{4g}$. The value for $g=0$ is from Table 1

$g \times 10^3$	Bo	δ	$\gamma \times 10^2$	θ
14	5.5 ± 1	4 ± 0.4	3.1 ± 0.6	50°
5.6	3.4 ± 0.6	5 ± 0.5	2.6 ± 0.5	57°
2.8	2.1 ± 0.5	5.5 ± 0.5	1.9 ± 0.5	63°
0.7	0.66 ± 0.25	7 ± 0.5	1.2 ± 0.4	66°
0.28	0.35 ± 0.2	7.2 ± 0.5	1.3 ± 0.3	70°
0	0	7.5 ± 0.6	1.1 ± 0.5	—

3.3. Comparison to experiment

To compare our results to experimental data for the surface tension of simple substances we employ an empirical model that has been shown [11] to fit this data. This model evaluates the surface free energy, ϕ , by integrating the Helmholtz free energy per particle, $\mu - pv$, across the tie line [11]

$$\phi = \frac{1}{3} \alpha(T) \int_{v_g(T)}^{v_l(T)} \frac{\mu - pv}{v^{5/3}} dv, \quad (7)$$

where v is the inverse number density and μ is the chemical potential. The coefficient $\alpha(T)$ effectively acts as a Jacobian relating the integration in length to the integration in volume, that is, $r = \alpha v^{1/3}$. This approach has been found to accurately fit experimental data for simple substances with $\alpha \approx 0.6$ [11] at all temperatures.

The surface tension is then obtained from the thermodynamic relation,

$$\gamma_e(T) = T \int_T^{T_c} \frac{\phi(T)}{T^2} dT. \quad (8)$$

Taking $\alpha(T) = 0.6$, the values of surface tension are listed in Table 1 and found to be in good agreement with the surface tension measured from the droplet pressure. This indicates that the vdW equation of state gives a reasonable surface tension for simple substances.

4. vdW theory of surface tension

Next, the results are compared to the celebrated van der Waals theory of surface tension. According to van der Waals the surface tension is given by [1]

$$\gamma_{vdW} = \int_0^\infty \left\{ F(n) + \frac{1}{2} m \left(\frac{dn}{dr} \right)^2 \right\} dr, \quad (9)$$

where $F(n)$ is the Gibbs free energy excess per unit volume as obtained from the difference between the chemical potential of the coexisting phases at temperature T ,

$\mu(T) = \mu_\ell(T) = \mu_v(T)$, and $M(n, T)$, the chemical potential within the vdW loop,

$$F(n) = \int_{n_\ell}^n [M(n, T) - \mu(T)] dn, \tag{10}$$

where $F(n_\ell) = F(n_v) = 0$. This theory has not been tested with the vdW equation of state since it requires knowledge of the density gradient through the interface and the coefficient m , which is discussed in the next section.

Estimates of the surface tension can be obtained (see Table 1) by utilizing the measured density gradient through the interface and exploiting the fact that the free energy reaches a minimum when the two terms in Eq. (9) contribute equally [1], thus requiring no knowledge of m . This leads to:

$$\gamma_{vdW} = \int_{n_v}^{n_\ell} 2 \frac{F(n)}{dn/dr} dn \approx \frac{2\delta}{n_\ell - n_v} \int_{n_v}^{n_\ell} F(n) dn. \tag{11}$$

The last numerical approximation is sufficiently precise in view of the uncertainty in the numerical results. The estimates obtained are consistent with the surface tension measurements using the Laplace equation and the model that reproduces experimental data. The results can also be summarized by quoting a value for m obtained by rewriting Eq. (9) as $m \approx \gamma_{vdW} \delta / (n_\ell - n_v)^2$, again using the fact that the two terms in Eq. (9) contribute equally. This leads to a temperature-independent estimate of $m = 0.8 \pm 0.2$.

5. Discussion

In the vdW mean field theory, m is identified with the second moment of the attractive part of the interaction potential $\Psi(r)$,

$$m = -\frac{1}{6} \int r^2 \Psi(r) d^3r. \tag{12}$$

This second moment diverges for long-ranged interaction potentials. This identification, in view of theoretical developments since vdW, is incomplete because the contribution to m from the constant long-range potential should vanish since all the particles always interact independent of their position, so the formation of the gradient requires no work. However, this term does not account for the work required to rearrange the reference hard sphere system to form the relatively steep density gradient, a quantity that can be obtained by separate molecular dynamics simulation for hard spheres [12]. The steep repulsive forces cannot be treated by mean field theory. Furthermore, the magnitude of the inhomogeneity present at the interface between the liquid and the vapor might violate the assumption that the expansion of the free energy functional only to second order suffices. However, close to the critical point where the interface thickness goes to infinity the truncation of the expansion should be acceptable but, as we know now through renormalization theory, the mean field theory is qualitatively wrong there.

We used our simulations to verify our original assertion that in the absence of fluctuations no interface is obtained (Section 2). We performed simulations where the displacement and the collision rate was not based on the local density but on the mean

field value, thus neglecting fluctuations in the spirit of mean field theory. In those simulations no phase separation was observed.

The simulation method allows verification of the vdW assertion that the existence of surface tension is related to the existence of an unstable loop of finite $\int F(n) dn$ area. When the equation of state, Eq. (2), is replaced with an equation of state that has a flat tie-line [4],

$$P_{TL}(n, T) = \begin{cases} P(n_v, T_v) = P(n_\ell, T_\ell), & n_v < n < n_\ell, \\ P(n, T) & \text{otherwise,} \end{cases} \quad (13)$$

no phase separation occurs even if density fluctuations are allowed. In this model the surface tension is zero since $F(n)=0$, that is, there is no compensating free energy gain to offset the cost of forming the inhomogeneity associated with the interface surface. We performed a gravity simulation ($g = 2.8 \times 10^{-3}$) using the flat tie-line equation of state (Eq. (13)) to verify this; although the fluid is forced to segregate into liquid and vapor regions to satisfy the equation of state and the hydrostatic condition

$$\nabla P = \rho \mathbf{g}, \quad (14)$$

the surface tension obtained is zero (-0.5 ± 0.5 from Eq. (6) with $\theta = 55^\circ$) to within the accuracy of the simulations.

6. Conclusions

The simulation results show that a stochastic particle simulation with a mean field attractive potential can capture the physics of phase separation and surface tension provided density fluctuations and an unstable vdW loop are allowed. This emphasizes the link between surface tension and mechanical stability in mean field approaches such as the vdW model and the DSMC algorithm.

In order to reproduce the value of m obtained from our simulations, separate molecular dynamics simulations of hard spheres must be performed to evaluate the contribution of the repulsive part of the potential to the work to form an interface gradient. These molecular dynamics simulations can also give an indication whether the free energy expansion needs to be continued to higher-order terms in the inhomogeneity. Further work involves the removal of the random displacement to reduce the uncertainties in the measurements. The simulation method presented here can also be used to generate the time evolution of droplet dynamics, such as droplet formation and coagulation.

Acknowledgements

The authors wish to thank F. Alexander, D. Rothman, J. Weeks, and B. Widom for enlightening discussions, and A. Shapiro for help with the computations. This

work is sponsored, in part, by the National Science Foundation and by the Department of Energy, contract W-7405-ENG-48 by Lawrence Livermore National Laboratory.

References

- [1] J.S. Rowlinson, B. Widom, *Molecular Theory of Capillarity*, Clarendon Press, Oxford, 1982.
- [2] J.L. Lebowitz, O. Penrose, *J. Math. Phys.* 7 (1966) 98.
- [3] F.J. Alexander, A.L. Garcia, B.J. Alder, *Phys. Rev. Lett.* 74 (1996) 5212.
- [4] F.J. Alexander, A.L. Garcia, B.J. Alder, *Physica A* 240 (1997) 196.
- [5] G.A. Bird, *Molecular Gas Dynamics*, Clarendon Press, Oxford, 1994.
- [6] F.J. Alexander, A.L. Garcia, *Comput. Phys.* 11 (1997) 588.
- [7] F.J. Alexander, A.L. Garcia, B.J. Alder, *J. Stat. Phys.* 89 (1997) 403.
- [8] F.J. Alexander, A.L. Garcia, B.J. Alder, *Phys. Fluids* 10 (1998) 1540.
- [9] P. Resibois, M. De Leener, *Classical Kinetic Theory of Fluids*, Wiley, New York, 1977.
- [10] R.C. Tolman, *J. Chem. Phys.* 17 (1949) 333.
- [11] A. Elsner, *Phys. Lett. A* 156 (1991) 147.
- [12] D.G. Triezenberg, R. Zwanzig, *Phys. Rev. Lett.* 28 (1972) 1183.
- [13] D.E. Sullivan, *Phys. Rev. A* 25 (1982) 3.
- [14] J.D. Weeks, D. Bedeaux, B.J.A. Zielinska, *J. Chem. Phys.* 80 (1984) 3790.